Electrochimica Acta 525 (2025) 146162

Contents lists available at ScienceDirect

Electrochimica Acta

journal homepage: www.journals.elsevier.com/electrochimica-acta

Single-step electrochemical fabrication of nanoporous gold film with reduced graphene oxide for carbendazim quantification in river water

Gilberto J. Silva Junior [a], Luiz F. Zavatti Felipe [a], Aline L. Muguet Pinto [b], Diele A. Gouveia Araújo [a], Thiago R.L.C. Paixão [a], Matias Regiart [c,*], Mauro Bertotti [a,*]

[a] Department of Fundamental Chemistry, Institute of Chemistry, University of São Paulo, Av. Prof. Lineu Prestes, 748, 05508-000, São Paulo, SP, Brazil
[b] Nuclear and Energy Research Institute (IPEN), University of São Paulo, Av. Prof. Lineu Prestes, 2242, 05508-000, São Paulo, SP, Brazil
[c] National University of San Luis, Faculty of Chemistry, Biochemistry and Pharmacy, Institute of Chemistry of San Luis, INQUISAL (CONICET), Chacabuco 917, San Luis, Argentina

ARTICLE INFO

Keywords:
Nanoporous gold electrode
Graphene oxide
Carbendazim
Pesticide detection
Environmental analysis

ABSTRACT

Carbendazim (CBZ) is a broad-spectrum fungicide used worldwide to control fungal infestations in various crops. However, its remarkable stability has raised concerns about accumulation in soils and aquatic environments, garnering significant attention from the analytical community. In this report, we propose a nanoporous gold electrode with reduced graphene oxide (NPGrGO) prepared according to a mold-assisted electrodeposition method, in which the gold film was deposited simultaneously with the reduction of graphene oxide on a gold microfiber surface for CBZ determination. The NPGrGO electrode exhibited a high density of edges with graphene sheets confined within the pores in the presence of gold nanoparticles. This unique configuration significantly enhances the electrochemical surface area and the roughness factor, directly influencing electrochemical measurements. Differential pulse voltammetry results show a linear behavior in the CBZ concentration range of 1 – 200 μmol L^{-1} with a limit of detection of 0.3 μmol L^{-1} and a limit of quantification of 1.0 μmol L^{-1}. Besides, the NPGrGO sensor also revealed excellent reproducibility (4.2 %), repeatability (3.7 %), and selectivity toward CBZ detection in the presence of other interfering molecules or ions. Finally, as proof of concept, the NPGrGO was used to determine CBZ in river water samples. Therefore, we have demonstrated a simple and rapid method for fabricating an NPGrGO electrochemical sensor, highlighting its significant potential for applications in environmental analysis.

1. Introduction

Carbendazim (CBZ) is a systemic fungicide with broad-spectrum activity, extensively employed globally for pre- and post-harvest applications to mitigate fungal infestations in citrus fruits, plants, and various crops, including beans, soybeans, and wheat [1–3]. It can also arise as a degradation product from other pesticides, such as methyl thiophanate and benomyl [4]. Known for its remarkable stability, CBZ exhibits persistent properties in both soil and aquatic environments, with an estimated half-life ranging from 3 days to 12 months [5]. With the increase in the planet's population and the escalation in food demand, the annual use of pesticides has risen significantly. Particularly in the case of CBZ, its application to soil results in long-lasting activity, often exhibiting slow degradation. Consequently, residues of this fungicide permeate water and soil extensively, posing substantial risks to human health and local aquatic ecosystems [6,7].

CBZ has a potential toxicity to humans, especially at high concentrations or prolonged exposure. This pesticide has been linked to adverse health effects such as infertility [8], kidney diseases [9], and an increase in liver cancer cases [10]. Its embryotoxic effects and role as an endocrine disruptor have raised significant public health concerns [11]. Consequently, numerous countries have banned CBZ use in agriculture or restricted its application to stringent regulatory standards.

CBZ determination has been reported using different analytical techniques, such as Fluorescence [12], Surface-enhanced Raman scattering [13], Liquid chromatography-mass spectrometry [14], Gas chromatography-mass spectrometry [15], and High-performance liquid chromatography-fluorescence [16], among others. These techniques present high sensitivity for CBZ detection, but they require sophisticated, bulky, and expensive equipment and often require lengthy

* Corresponding authors.
E-mail addresses: matiasregiart@gmail.com (M. Regiart), mbertott@iq.usp.br (M. Bertotti).

https://doi.org/10.1016/j.electacta.2025.146162
Received 13 December 2024; Received in revised form 19 March 2025; Accepted 31 March 2025
Available online 1 April 2025

analysis times, making field monitoring unfeasible. Hence, the development of electrochemical sensors for CBZ detection is interesting, as they are cheap, highly sensitive, and can be miniaturized easily without damaging the detectability and selectivity, which allows real-time and portable analysis.

A simple and effective strategy to improve electroanalytical methods' sensitivity and selectivity is modifying the electrode surface using porous materials due to their unique properties, such as high surface, electrical conductivity, stability, and catalytic effects [17]. For instance, nanoporous gold (NPG) materials have been prepared by various methods and extensively used for several applications [18–22]. High surface area noble metal electrodes have been fabricated through different approaches, including chemical and electrochemical dealloying [23,24], anodization [25,26], electrodeposition with H_2 bubble formation [27,28], etc. Each one has its unique advantages, but special attention has been given to the method known as the Dynamic Hydrogen Bubble Template (DHBT), which uses the formation of H_2 bubbles as a template for metal deposition [29]. It is possible to optimize parameters such as precursor concentration, potential, and deposition time from mold-assisted electrodeposition, which ensures the best control of the nanoporous film characteristics [30].

Previous studies show that researchers in this field have made efforts to fabricate hybrid films containing gold-based nanomaterials [31,32] and gold nanostructured films with carbonaceous materials [33–36]. Among carbon materials, graphene oxide (GO) stands out in sensing organic molecules due to its attractive properties, such as large specific surface area, chemical stability, homogeneity, and good geometrical arrangement when incorporated into metallic films. Also, the excellent electrical conductivity makes it a promising candidate for many applications [37,38]. There are different ways to obtain graphene oxide films. In most cases, an additional step is required to promote the reduction of the material and get the reduced graphene oxide (rGO) for electroanalytical determinations [39–41].

Herein, we present a novel method for the electrochemical determination of CBZ through simultaneous electrodeposition of a nanoporous gold film on the electrode surface and reduced graphene oxide. We also demonstrate that this platform significantly enhances the electrochemical surface area and catalytic activity, which is an important issue considering the development of a sensitive and selective sensor for CBZ detection in natural water samples. To our knowledge, this is the first report on the preparation of a platform for CBZ detection based on nanoporous gold film and reduced graphene oxide.

2. Experimental section

2.1. Chemicals

Carbendazim (CBZ), hydrogen tetrachloroauric (III) trihydrate ($HAuCl_4{\cdot}3H_2O$), and graphene oxide flakes were purchased from Sigma-Aldrich. Sulfuric acid (H_2SO_4), acetic acid (H_3CCOOH), phosphoric acid (H_3PO_4), and boric acid (H_3BO_3) were acquired from Merck. All the reagents were analytical grade and used without further purification unless otherwise stated. The solutions were prepared using milli-Q-water with 18.0 MΩ cm resistivity.

2.2. Instrumentation

All the electrochemical measurements were performed using an AUTOLAB PGSTAT128N potentiostat interfaced with Nova 1.11 software. The experiments were carried out in a three-electrode configuration cell, using gold microelectrode (Au), Ag/AgCl (saturated KCl), and platinum wire as the working, reference, and auxiliary electrodes. The gold microelectrode was polished using sandpaper (Grit 600 and 1200). Then, cyclic voltammograms were recorded in 0.5 mol L^{-1} H_2SO_4 solution to ensure the microelectrode worked adequately. The pH of the solutions was adjusted using a pHmeter model 827 pH labs (Metrohm). Surface morphology images of the nanoporous gold were taken by field emission-scanning electron microscopy using a JOEL JSM-7401F (30 kV) FE-SEM equipment. Raman measurements were carried out with a high-resolution WITec 300-R confocal microscope. The samples were scanned with a laser within an area of 1.8 μm^2 and a CCD detector of 1600 × 200 pixels. The He-Ne LASER wavelength, power, and integration time were 633 nm, 20 mW, and 1 s, respectively.

2.3. Fabrication of gold microelectrode

A gold microelectrode was fabricated using a gold fiber ($\varnothing = 25$ μm) and a micropipette tip (capacity of 200 μL), and Figure SM1 illustrates the fabrication steps. Initially, the gold fiber was glued to a nickel-chromium wire using a glue silver conductor. Then, the fiber was placed at the narrowest tip of the pipette tip and sealed using Araldite (Tekbond) epoxy glue. The tip was placed in a well-ventilated space to facilitate drying. When the glue was completely dry, the micropipette tip was filled with carbon black. Although the fiber was bonded to the nickel-chromium wire, filling the pipette with conductive material is essential to ensure electrical contact. Finally, the other end of the tip was sealed using Parafilm (Merck). The microelectrode was polished using sandpaper (Grit 600) to remove the excess glue. Afterward, the surface of the microelectrode was polished with sandpaper (Grit 1200), and a $\varnothing = 25$ μm fiber disc was exposed. Finally, the microelectrode surface was copiously washed with distilled water.

2.4. Preparation of nanoporous gold with reduced graphene oxide

A single-step amperometric method was employed to prepare a nanoporous gold electrode with reduced graphene oxide (NPGrGO). The modification was performed through an electrodeposition with H_2 bubbles (DHBT) by applying −4 V for 250 s. The electrochemical cell was composed of three electrodes immersed in 4 mL of a 5 mmol L^{-1} $HAuCl_4$ solution in an acid medium (0.5 mol L^{-1} H_2SO_4) containing 1 mg of commercial graphene oxide (Sigma Aldrich). The precursor solution was previously sonicated for 10 min to obtain homogeneity. Electrodeposition was performed with constant stirring using a magnetic bar under the working electrode to release the H_2 bubbles formed during the modification. The parameters of the modification step, such as the applied potential, the deposition time, and the concentration of graphene oxide, were previously optimized. A nanoporous gold microelectrode was prepared using the same protocol but without graphene oxide (NPG) for a comparative study.

2.5. Pretreatment of river water samples

River water samples were collected in pre-cleaned amber glass bottles (1000 mL) from the Pinheiros River (geographic coordinates: −23.554410, −46.723980) in São Paulo, Brazil. The sample bottles were transported in an ice cooler to the laboratory and kept at 4 °C until the analysis to prevent the proliferation of microorganisms in the sample. The pH of the collected water was 6.93. Further, the samples were filtered through Millipore mixed cellulose ester membrane filters (0.5 μm pore size).

2.6. Analytical parameters for CBZ determination

The analytical curve was obtained in a 5 to 250 μmol^{-1} CBZ concentration range in 0.04 mol L^{-1} BR Buffer solution (pH 7.0) using the differential pulse voltammetry (DPV) technique. The CBZ electrochemical response was recorded in the potential range from 0.7 to 1.3 V (vs. Ag/AgCl sat KCl), and the optimized parameters were determined as pulse amplitude 50 mV, step potential 5 mV, and scan rate 50 mV s^{-1}. Five replicates of each concentration were performed to estimate the precision.

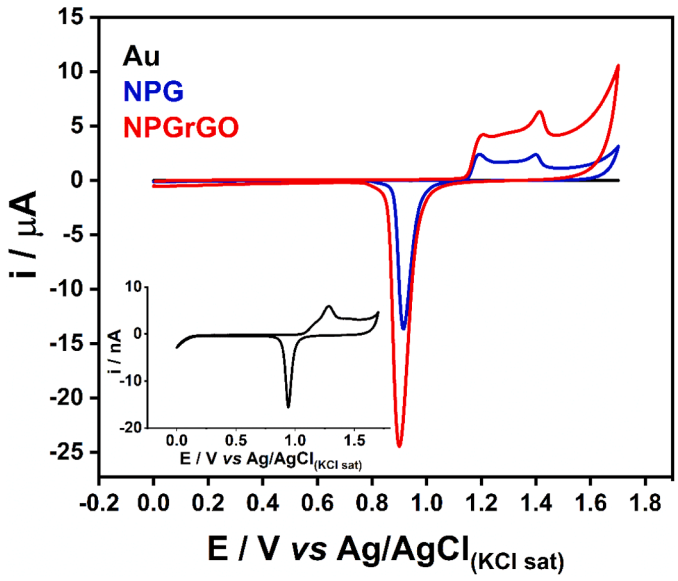

Fig. 1. CVs recorded in a 0.5 mol L^{-1} H_2SO_4 solution using bare Au, NPG, and NPGrGO microelectrodes. Inset: Amplified CV recorded with the bare Au microelectrode. Scan rate: 100 mV s^{-1}.

3. Results and discussion

3.1. Electrochemical and morphological characterization

The electrochemical characterization was performed by comparing the electrochemical behavior of three electrodic surfaces: bare gold microelectrode (Au), NPG, and NPGrGO. Fig. 1 shows typical cyclic voltammograms for these electrodes recorded in a 0.5 mol L^{-1} H_2SO_4 solution. Because of the larger surface area, nanoporous surfaces substantially enhance anodic and cathodic currents. For instance, a 2500-fold increase in the cathodic peak current ($E = +0.9$ V) was observed for the NPGrGO sensor compared to the bare Au microelectrode, while the NPG electrode showed a 1400-fold increase. This increase can be attributed to two fundamental mechanisms. Firstly, the hydrogen bubbles act as a template, facilitating the creation of the nanoporous film. Secondly, graphene sheets, confined within these pores, could act as scaffolds for the deposition of gold nanoparticles. This dual mechanism enhances the electrochemical surface area (ECSA) significantly compared to the nanoporous gold (NPG) electrode, which relies solely on the formation of hydrogen bubbles. ECSA values of all electrodes were calculated from the corresponding charge of the Au oxide reduction peak by the charge-integration method [25], and the results are given in Table SM1. These results confirm the NPGrGO presents a large surface area.

Subsequently, the NPGrGO electrode was characterized using a well-known electrochemical probe solution to infer whether the proposed modification method would require an additional electrochemical step to ensure the reduction of graphene oxide. In this study, the NPGrGO electrode was compared to another electrode submitted to a further treatment step generally used to promote the reduction of graphene oxide. In this sense, after the electrode modification step, the treated NPGrGO electrode was cycled 10 times in a deaerated 50 mmol L^{-1} Na_2SO_4 solution. The potential window in the additional step was from 1.0 to −1.0 V at 50 mV s^{-1}. Figure SM2 shows the CVs obtained in a 5 mmol L^{-1} $K_3[Fe(CN)_6]$ in 0.1 M KCl at 50 mV s^{-1} using the NPGrGO and the treated NPGrGO. The results show that the surface modification protocol proposed in the present work promoted the formation of a nanoporous gold film and the simultaneous reduction of graphene oxide. This conclusion is supported by an analysis of the identical voltammetric profiles obtained for the NPGrGO microelectrodes (with and without the additional treatment step). Figure SM2 (inset) illustrates the CV results for the bare Au microelectrode, which exhibited a sigmoidal profile consistent with the expected for a polished bare gold microelectrode. By comparing the voltammograms presented in Figure SM2, one can also notice a current increase for the NPG microelectrodes compared to the bare one and the change in the voltammetric profile. However, such a current enhancement is not proportional to the ECSA increase because ferricyanide's electron transfer process is very fast; hence, not all interior pores are employed in the electrochemical process.

The morphological characterization of all surfaces was performed using Field Emission Scanning Electron Microscopy (FE-SEM) images (Fig. 2). Fig. 2a illustrates the bare Au microelectrode with a highly smooth and planar surface. Minor grooves may be present, contingent on the polishing procedure applied. Fig. 2b depicts the morphology of the nanoporous gold (NPG) electrode, which features a three-dimensional network with small pores and interconnected ligaments. Upon further magnification (Fig. 2c), it is evident that the NPG electrode displays porous dendritic structures on a denser layer. The enhancement of these hierarchical structures could lead to the formation of new active sites. The electrodeposition parameters (potential and deposition time) significantly affect the structure of the resulting porous film and, consequently, can impart varied physicochemical properties to the electrode [42]. The surface of the NPGrGO electrode exhibited a highly porous structure, resembling a metallic foam with pores of varying sizes, similar to the NPG electrode. However, for higher magnifications (Fig. 2d), it is possible to observe an increase in the dendritic structures and the graphene sheets deposited on the gold film or still confined within the pores. Fig. 2e shows the deposited graphene sheets that act as a substrate for the electrodeposition of gold nanoparticles. When the image is magnified (Fig. 2f), it becomes increasingly apparent that the gold nanoparticles exhibited substantial growth on the graphene sheets situated on the film. This observation accounts for the considerable increase in peak current observed with the NPGrGO electrode, which may enhance the detectability in analytical applications.

The Raman spectra for bare and modified electrodes are depicted in Figure SM3. The bare Au (red line) and NPG (black line) electrodes exhibit no discernible bands, indicating that these materials are predominantly pure gold. Conversely, the NPGrGO (blue line) electrode reveals distinct D and G bands centered at 1337 cm^{-1} and 1600 cm^{-1}, respectively [43]. These observations confirm that synthesizing the nanoporous film with reduced graphene oxide using a single-step amperometric method was both effective and easy to implement.

3.2. CBZ electrochemical behavior

CBZ electrochemical behavior on bare Au and nanoporous surfaces was evaluated by cyclic voltammetry using a 150 μmol L^{-1} CBZ solution in 0.04 mol L^{-1} BR buffer (pH 7). The CVs were recorded in a potential range from 0.7 to 1.3 V at a scan rate of 50 mV s^{-1}, as shown in Fig. 3. We established a pH of 7.0 to avoid manipulating the sample, given that the developed electrode will be applied for river water analyses. Previous methods reported in the literature support the selection of a neutral medium for the electrochemical detection of CBZ [44,45].

Fig. 3a compares the voltammetric signals recorded with a bare Au electrode in both the absence and presence of the analyte. In the presence of CBZ, although the electrode presented a voltammetric profile distinct from the background current, no anodic peak was detected. In contrast, when electrodes with nanoporous surfaces were utilized, a defined peak corresponding to the oxidation of CBZ was observed at $E = +1.2$ V. Fig. 3b presents the CVs for bare Au and both NPG and NPGrGO electrodes. The NPG electrode exhibits an oxidation peak for CBZ, indicating that the nanoporous film imparts an electrocatalytic effect, which is not observed with the bare Au microelectrode. According to the literature [46,47], the anodic peak can be attributed to an electrochemical irreversible conversion of the amino group to a nitro group (–NO), as described below:

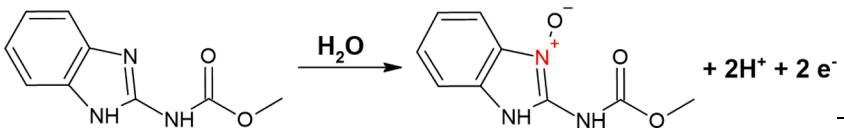

An even more significant improvement was observed for the NPGrGO electrode since the peak profile was better defined, and the current obtained was about 5000-fold higher than that of the NPG electrode at 1.2 V. The synergistic effect between the nanoporous film and the reduced graphene oxide is responsible for such behavior. Incorporating graphene sheets into the film facilitates the electrodeposition of gold nanoparticles onto these sheets and enhances the formation of new active sites, significantly improving CBZ's electron transfer. For comparative purposes, the electrochemical behavior of CBZ was also assessed using a graphene oxide-modified electrode in the absence of gold (rGO electrode). CV was performed under the same conditions as described above, with the results presented in Figure SM4. As shown, CBZ exhibits a discrete oxidation peak at $E = +1.2$ V. However, the current response is comparable to that of the polished gold electrode, suggesting that the surface modification does not significantly enhance the electrochemical behavior. Therefore, it is apparent that the key factor contributing to the enhanced anodic oxidation of CBZ is the interaction between the graphene oxide layers and the nanoporous gold film, which together impart superior electrochemical performance to the NPGrGO electrode. Consequently, the NPGrGO electrode is a promising

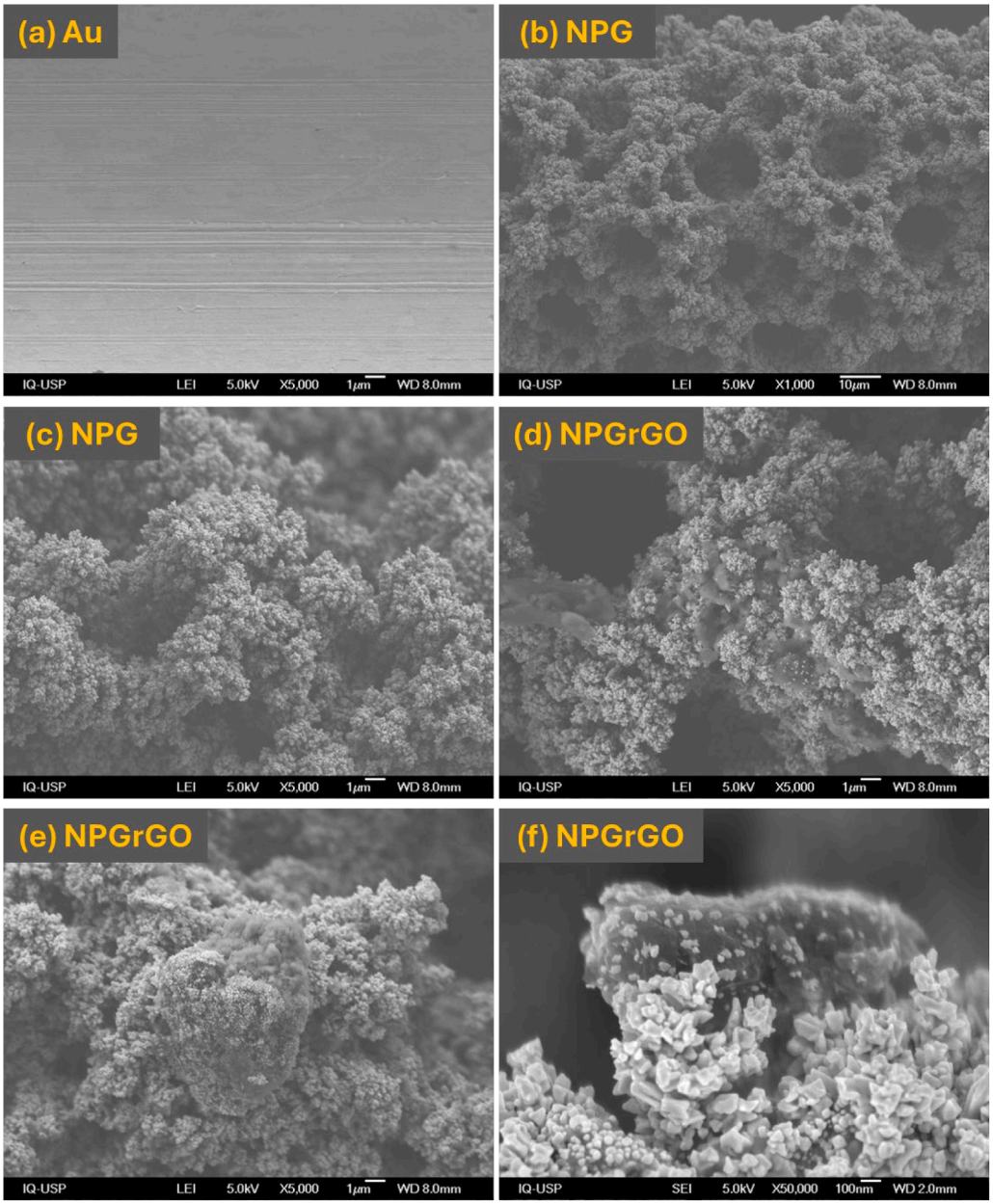

Fig. 2. SEM images of the surface of bare Au (a), NPG (b, c), and NPGrGO (d-f) microelectrodes at different magnifications.

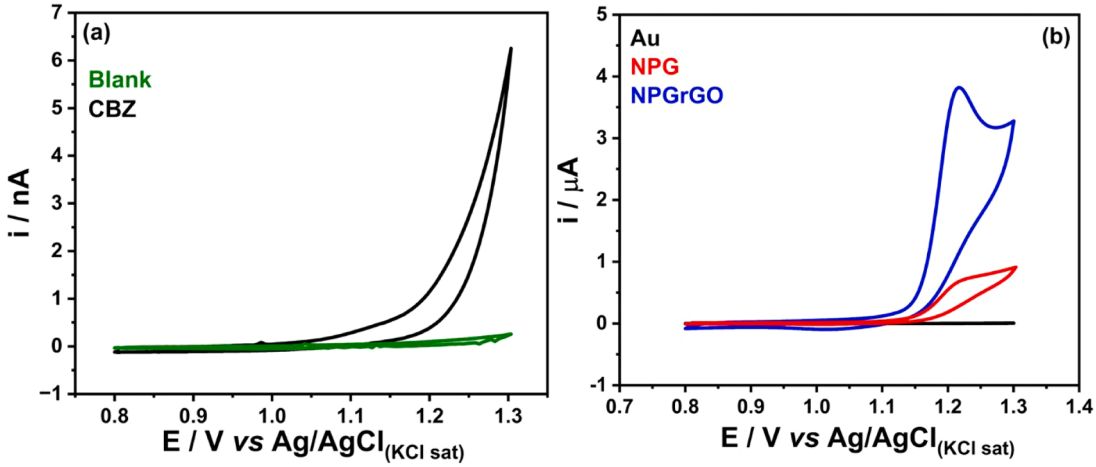

Fig. 3. CVs recorded in a 0.04 mol L^{-1} BR Buffer solution at pH 7.0 in the presence and absence of 150 µmol L^{-1} CBZ using a bare Au microelectrode (a) and CVs recorded in a 250 µmol L^{-1} CBZ in 0.04 mol L^{-1} BR Buffer (pH 7.0) using bare Au, NPG and NPGrGO microelectrodes (b). Scan rate: 50 mV s^{-1}.

platform for sensitively detecting the CBZ fungicide in aqueous samples.

3.3. Optimization of NPGrGO fabrication

Some important parameters of the modification step were optimized to obtain the most suitable NPGrGO film for developing a CBZ sensing: potential, deposition time, and graphene oxide concentration. All studies were conducted using univariate analysis, where one parameter was varied while all others remained fixed. Fig. 4 shows the results obtained by differential pulse voltammetry in 4 mL of a solution containing 1 mmol L^{-1} CBZ in 0.04 mol L^{-1} BR Buffer (pH 7.0) using sensors fabricated by applying different potentials (- 1, - 2, - 3, and −4 V). Fig. 4a

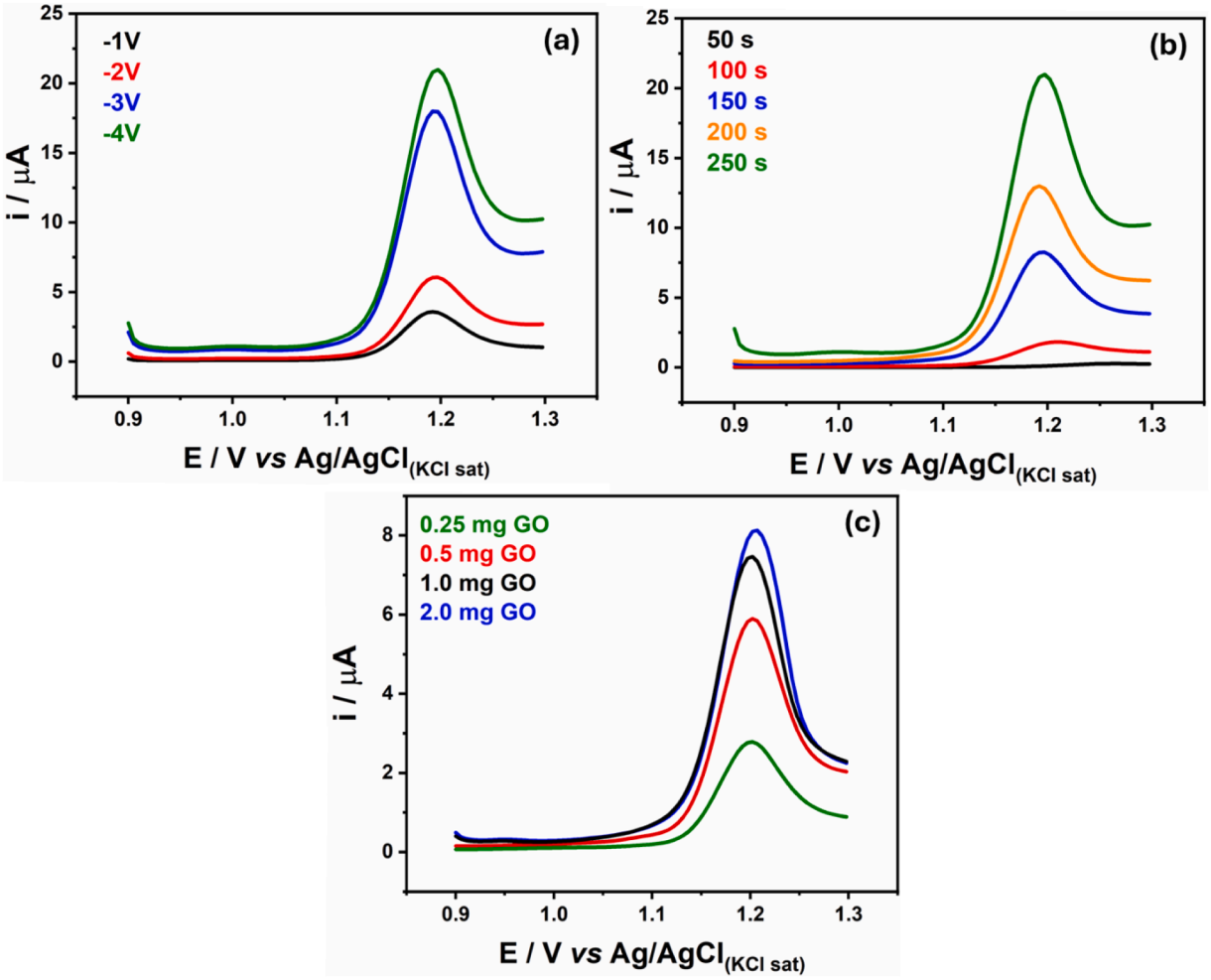

Fig. 4. DPVs recorded in a 250 µmol L^{-1} CBZ solution in 0.04 mol L^{-1} BR Buffer (pH 7.0) using an NPGrGO electrode fabricated at different potentials (a), different deposition times (b), and different graphene oxide concentrations (c).

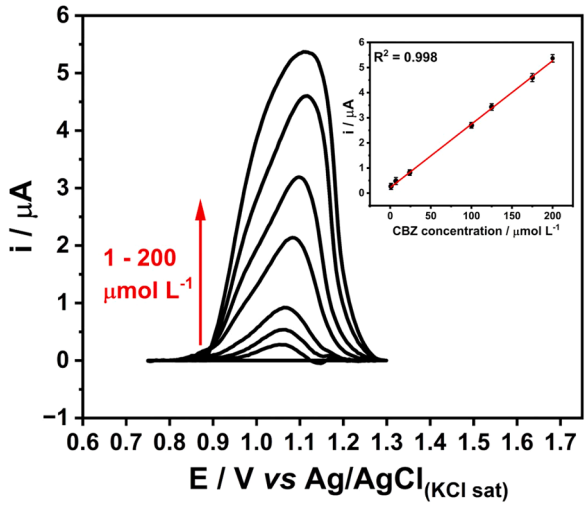

Fig. 5. DPVs of CBZ at various concentrations (1 to 200 μmol L^{-1}) in 0.04 mol L^{-1} BR Buffer solution (pH 7.0) using the NPGrGO electrode (a); Corresponding calibration plot (b).

shows DPVs recorded with the NPGrGO prepared at a fixed time (250 s) and using 0.5 mg of graphene oxide dispersed in a 5 mmol L^{-1} $HAuCl_4$ + 0.5 mol L^{-1} H_2SO_4 solution. The anodic current corresponding to the CBZ oxidation increases as the potential becomes more negative. Although there is no significant difference between the results obtained for −3 and −4 V, −4 V was defined as the optimal potential. Afterward, the NPGrGO electrode was fabricated by applying the optimized potential at different electrodeposition times (50, 100, 200, 250, and 300 s). As one can see, longer deposition times result in a higher peak current, suggesting a larger surface area. However, after 250 s, the current intensity reached a plateau, indicating that the electrode surface was saturated. Thus, the time employed for the modification step was set to 250 s (Fig. 4b). Finally, the amount of commercial graphene oxide (0.25, 0.50, 1.0, and 2.0 mg) dispersed in the 4 mL of the gold precursor solution was optimized. Fig. 4c presents the DPVs obtained for the NPGrGO material synthesized with different graphene oxide concentrations. When the concentration of graphene oxide exceeded 1.0 mg dispersed in 4 mL of the gold precursor solution, the peak current remained stable without further variations. Therefore, the NPGrGO electrode was prepared by applying a potential of −4 V for 250 s in a 5 mmol L^{-1} $HAuCl_4$ + 0.5 mol L^{-1} H_2SO_4 solution containing 1.0 mg of commercial graphene oxide.

3.4. Analytical performance

The analytical performance for CBZ quantification was evaluated using the NPGrGO electrode in a 0.04 mol L^{-1} BR Buffer solution (pH 7) at various CBZ concentrations in the 1 to 200 μmol L^{-1} range. Fig. 5 shows DPV curves using optimized parameters (pulse amplitude of 50 mV and step potential of 5 mV), and current values proportional to CBZ concentration are observed according to the equation: i(μA) = 0.0253 + 0.0222 C_{CBZ} (μmol L^{-1}) (R^2 = 0.998). The limit of detection (LOD) and limit of quantification (LOQ) were calculated according to IUPAC recommendations, and the found values were 0.3 and 1.0 μmol L^{-1}, respectively. Notably, the found LOD is below the maximum residue limit (MRL) for CBZ in water samples established by the Australian Environmental Protection Agency (0.5 μmol L^{-1}). This threshold is one of the few environmental rules that still allow the controlled use of this ingredient in crop protection products [48].

A comparison of some analytical parameters for CBZ determination using the NPGrGO electrode and sensors reported in the literature is presented in Table 1. The developed sensor is more sensitive than those listed in the table, even though one of those works reported a lower LOD. However, the proposed NPGrGO sensor can be fabricated in minutes, not depending on laborious steps such as layer-by-layer modification [52, 53]. In addition, the developed NPGrGO does not require biomolecules [54], which makes the process cheaper and with simple manipulation of the materials used as modifiers of the electrode surface.

Repeatability and reproducibility were also evaluated. A within-assay precision study was assessed by detecting different CBZ concentrations (10, 25, 50, and 100 μmol L^{-1}) in five continuous tests on the same day and using the same electrode. These measurements were repeated for three consecutive days to estimate the between-assay precision. The results are presented in Table 2 and confirm that the NPGrGO sensor presented excellent precision since the RSD values of within-assay and between-assay measurements were below 3.7 % and 4.0 %, respectively. The reproducibility of the sensor was calculated by recording DPVs in a 1 μmol L^{-1} CBZ solution with five different NPGrGO electrodes. The relative standard deviation (RSD) of 4.2 % indicates the sensor fabrication is reproducible. The fabricated NPGrGO electrode was stored in a vial containing 0.5 mol L^{-1} H_2SO_4 to ensure the electrode's stability. The studies were repeated every three days, and the platform remained stable without significant variations for 21 days (current variation < 4.7 %).

A recovery study was performed to assess the applicability of the NPGrGO sensor for quantifying CBZ in river water samples. The study employed the standard addition method using DPV. The river sample was enriched with 1 μmol L^{-1} of the pesticide (base concentration), and successive concentrations were added to evaluate the percentage recovery of the electrode. The NPGrGO sensor demonstrated high accuracy without interference from the sample matrix (Table 3). These results suggest that the NPGrGO sensor is a practical approach for CBZ quantification in river water samples.

The selectivity of the sensor for detecting CBZ in the presence of potential interferents commonly used in crop protection products was also thoroughly evaluated. In these studies, the concentration of the interfering species was fixed at a 30-fold higher than that of CBZ (1 μmol L^{-1}). From the results in Fig. 6, one can conclude that none of the tested species significantly affected the CBZ determination, with interference remaining below 5 %. These results suggest that the synergistic effect of the nanoporous gold film and reduced graphene oxide sheets enhances

Table 1
Comparison of different modified electrodes and electroanalytical techniques for CBZ.

Surface	Technique	Linear range / μmol L^{-1}	LOD / μmol L^{-1}	Stability	Sample	Ref.
β-CD-MWCNTs-BDDE	SWAdSV	0.7 - 11.2	0.27	Not informed	River water	[49]
Laser induced graphene	SWV	1.0 - 40	0.67	5 days	Wastewater	[50]
BDD	SWV	5.0 - 69	1.6	Not informed	Lemon juice	[51]
Carbon fiber	DPV	0.1 – 2.0	2.6	30 days	Soil	[52]
CCME	DPV	0.08 – 2.0	0.02	Not informed	Mango juice	[53]
NPGrGO	DPV	1.0 - 200	0.3	21 days	River water	This work

SWAdSV: Square Wave Adsortive stripping voltammetry.
SWV: Square Wave Voltammetry.
DPV: Differential Pulse Voltammetry.

Table 2
Within-assay precision and between-assay precision for the NPGrGO electrode.

Sample*	Within-assay	Between-assay
1	0.92 ± 0.03	1.17 ± 0.05
5	5.2 ± 0.2	5.2 ± 0.2
10	10.1 ± 0.3	9.8 ± 0.4
25	25 ± 1	25 ± 1
50	50 ± 2	50 ± 2

* μmol L^{-1}.

Table 3
Recovery study of CBZ in spiked river water samples (95 % confidence interval; n = 5).

Base[a]	Added	Found	Recovery[b]
1	–	1.1 ± 0.2	–
1	4	5.2 ± 0.2	105
1	10	10.8 ± 0.1	98
1	25	26.4 ± 0.6	101.6
1	50	52 ± 1	102

[a] μmol L^{-1}.
[b] Recovery = [(found-base)/added] × 100.

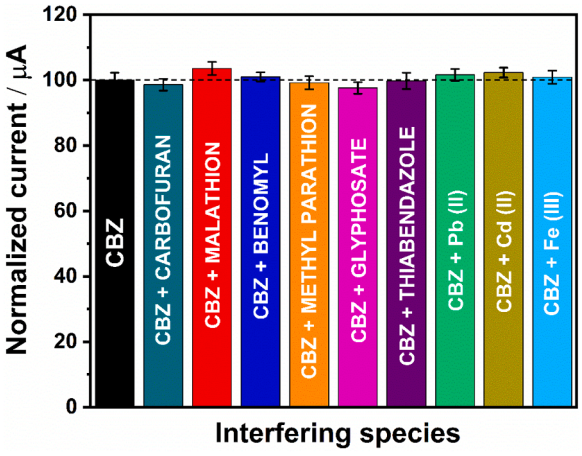

Fig. 6. Interference study performed in solutions containing 250 μmol L^{-1} CBZ in absence and presence (30-fold concentration) of some interfering substances using the NPGrGO electrode.

the rate of electron transfer, resulting in increased sensitivity and improved selectivity.

4. Perspectives

To further enhance the detection of pesticides in water resources using modified electrodes, the combination of reduced graphene oxide with other nanostructured metals, such as platinum or palladium, could be explored. This approach has the potential to enable the simultaneous detection of multiple contaminants. Additionally, the development of disposable paper-based sensors could be pursued by modifying the electrode surface through pulsed laser deposition or nanomaterial printing techniques. This would significantly improve sensor portability and enable more efficient in-situ analysis. Future studies could focus on the systematic optimization of electrode surface functionalization, including the modulation of particle size or the incorporation of specific functional groups or biomolecules to selectively interact with a broader range of target analytes.

5. Conclusions

This work presents a facile and rapid method for fabricating an electrochemical sensor modified with a nanoporous gold film electrodeposited with reduced graphene oxide. The optimized material was prepared using a single-step amperometric method, and the nanostructured sensors exhibited a more suitable surface for the anodic oxidation of CBZ, as no evident response for this compound was observed using a bare Au microelectrode. In addition, combining the nanoporous gold film with graphene oxide resulted in a remarkable sensitivity enhancement. This synergy increased the electroactive surface area, creating a hybrid material composed of nanoporous gold, gold nanoparticles, and reduced graphene oxide. The morphological characterization studies confirmed the composition of the prepared film. As proof of concept, the sensor was used to quantify CBZ in river water samples using a simple preparation step, and a recovery close to 100 % was found. Therefore, we have demonstrated a simple and rapid method for fabricating the NPGrGO electrode, highlighting its significant potential for applications in environmental analysis.

CRediT authorship contribution statement

Gilberto J. Silva Junior: Writing – original draft, Methodology, Investigation, Formal analysis, Data curation, Conceptualization. **Luiz F. Zavatti Felipe:** Writing – review & editing, Methodology, Formal analysis, Data curation. **Aline L. Muguet Pinto:** Methodology, Formal analysis, Data curation. **Diele A. Gouveia Araújo:** Investigation, Formal analysis, Data curation. **Thiago R.L.C. Paixão:** Writing – review & editing, Visualization, Supervision, Resources, Project administration, Investigation. **Matias Regiart:** Writing – review & editing, Methodology, Investigation, Conceptualization. **Mauro Bertotti:** Writing – original draft, Supervision, Project administration, Methodology, Funding acquisition.

Declaration of competing interest

The authors declare that they have no known competing financial interests or personal relationships that could have appeared to influence the work reported in this paper.

The authors declare in manuscript the financial interests/personal relationships which may be considered as potential competing interests.

Acknowledgments

The authors would like to thank the financial support from the São Paulo State Research Foundation (FAPESP 2019/14418-3, 2023/00246-1, 2022/00064-8, 2022/01810-5, 2019/06293-6), the National Council for Scientific and Technological Development (CNPq 103418/2024-5), and the Consejo Nacional de Investigaciones Científicas y Técnicas (CONICET, Argentina). We also acknowledge Dr. Helton Pereira Nogueira for helping us obtain Raman spectra.

Supplementary materials

Supplementary material associated with this article can be found, in the online version, at doi:10.1016/j.electacta.2025.146162.

Data availability

Data will be made available on request.

References

[1] A.C.M. Oliveira, D.A.G. Araújo, L.A. Pradela Filho, et al., A robust and versatile micropipette tip-based miniaturized electrochemical cell for determination of carbendazim, Sens. Actuators B Chem. 327 (2021) 128880.
[2] S. Xue, J. Zou, J. Li, et al., Electrochemical detection of carbendazim using molecularly imprinted poly(3,4-ethylenedioxythiophene) on Co,N co-doped hollow carbon nanocage@CNTs-modified electrode, Food Chem. 456 (2024) 140063.
[3] A. Zengim, Y. Toptas, M. Bilici, T. Gursoy, A molecularly imprinted cotton fabric for rapid, selective and sensitive determination of carbendazim in orange juice, J. Food Compos. Anal. 133 (2024) 106480.

[4] Y. Yang, H. Tan, Y. Wang, et al., A novel electrochemical sensor for sensitive detection of carbendazim based on zeolitic-imidazolate-framework-67/carbon nanohorns nanocomposite, Mater. Res. Bull. 179 (2024) 112975.
[5] R.D. Crapnell, P.S. Adarakatti, C.E. Banks, Electroanalytical overview: the sensing of carbendazim, Anal. Methods 15 (2023) 4811.
[6] S.D. Mechannavar, M.M. Shanbhag, M.A. Alshehri, N.P. Shetti, Mesoporous pineapple crown-derived activated carbon modified matrix for the detection of carbendazim in the presence of anionic surfactant, Diam. Relat. Mater. 148 (2024) 111352.
[7] C. Tian, S. Zhang, H. Wang, et al., Three-dimensional nanoporous copper and reduced graphene oxide composites as enhanced sensing platform for electrochemical detection of carbendazim, J. Electroanal. Chem. 847 (2019) 113243.
[8] T. Zhou, T. Guo, Y. Wang, et al., Carbendazim: ecological risks, toxicities, degradation pathways and potential risks to human health, Chemosphere 314 (2023) 137723.
[9] Y.A. Ebedy, M.O. Elshazly, N.H. Hassan, Novel insights into the potential mechanisms underlying carbendazim-induced hepatorenal toxicity in rats, J. Biochem. Mol. Toxicol. 36 (8) (2022) e23079.
[10] F. Beigmoradi, M.R. Moghadam, A. Bazmandegan-Shamili, H.R. Massodi, Electrochemical sensor based on molecularly imprinted polymer coating on metal–organic frameworks for the selective and sensitive determination of carbendazim, Microchem. J. 179 (2022) 107633.
[11] X.B. Joseph, J.N. Baby, S. Wang, et al., Interfacial superassembly of Mo2C@NiMn-LDH frameworks for electrochemical monitoring of carbendazim fungicide, ACS Sustain. Chem. Eng. 9 (44) (2021) 14900–14910.
[12] W. Guo, Y. Fu, S. Liu, et al., Multienzyme-targeted fluorescent probe as a biosensing platformfor broad detection of pesticide residues, Anal. Chem. 96 (18) (2021) 7079–7085.
[13] J. Shi, C. Li, Z. Jiang, A new nanosurface molecularly imprinted polymer difunctional probe and on-site generated gold nanosol SERS/RRS/Abs trimode determination of trace carbendazim, Microchem. J. 196 (2024) 109573.
[14] A. Gamal, M. Soliman, M.S. Al-Anany, F. Eissa, Optimization and validation of high throughput methods for the determination of 132 organic contaminants in green and roasted coffee using GC-QqQ-MS/MS and LC-QqQ-MS/MS, Food Chem. 449 (2024) 139223.
[15] A.Y. Hamadamin, K.I. Hassan, Gas chromatography–mass spectrometry based sensitive analytical approach to detect and quantify non-polar pesticides accumulated in the fat tissues of domestic animals, Saudi J. Biol. Sci. 27 (3) (2020) 887–893.
[16] S.D. Regis-Rolle, G.M. Bauville, High-performance liquid chromatographic method for the determination of carbendazim residues in crops, grains, and wines with fluorescent detection, Pestic. Sci. 37 (3) (1993) 273–282.
[17] J. Patel, L. Radhakrishnan, B. Zhao, et al., Electrochemical properties of nanostructured porous gold electrodes in biofouling solutions, Anal. Chem. 85 (23) (2013) 11610–11618.
[18] E. Seker, M. Reed, M. Begley, Nanoporous gold: fabrication, characterization, and applications, Materials 2 (2009) 2188–2215.
[19] A. Wittstock, A. Wichmann, M. Bäumer, Nanoporous gold as a platform for a building block catalyst, ACS Catal. 2 (2012) 2199–2215.
[20] J. van der Zalm, S. Chen, W. Huang, A. Chen, Review-recent advances in the development of nanoporous Au for sensing applications, J. Electrochem. Soc. 167 (2020) 037532.
[21] G.J. Silva Junior, J.S.G. Selva, A. Sukeri, et al., Fabrication of dendritic nanoporous gold via a two-step amperometric approach: application for electrochemical detection of methyl parathion in river water samples, Talanta 226 (2021) 122130.
[22] A. Kumar, V.L. Furtado, J.M. Gonçalves, et al., Amperometric microsensor based on nanoporous gold for ascorbic acid detection in highly acidic biological extracts, Anal. Chim. Acta 1095 (2020) 61–70.
[23] F.L. Jia, C.F. Yu, K.J. Deng, L.Z. Zhang, Nanoporous metal (Cu, Ag, Au) films with high surface area: general fabrication and preliminary electrochemical performance, J. Phys. Chem. C 111 (24) (2007) 8424–8431.
[24] F. Meng, X. Yan, J. Liu, J. Gu, Z. Zou, Nanoporous gold as non-enzymatic sensor for hydrogen peroxide, Electrochim. Acta 56 (2011) 4657–4662.
[25] A. Sukeri, L.P.H. Saravia, M. Bertotti, A facile electrochemical approach to fabricate a nanoporous gold film electrode and its electrocatalytic activity towards dissolved oxygen reduction, Phys. Chem. Chem. Phys. 17 (2015) 28510–28514.
[26] R.S.O. Lins, A. Sukeri, M. Bertotti, A home-made nanoporous gold microsensor for lead(ii) detection in seawater with high sensitivity and anti-interference properties, Anal. Methods 16 (2024) 4415–4420.
[27] W. Huang, M. Wang, J. Zheng, Z. Li, Facile fabrication of multifunctional three-dimensional hierarchical porous gold films via surface rebuilding, J. Phys. Chem. C 113 (5) (2009) 1800–1805.
[28] A. Sukeri, E.J. de Carvalho Junior, M. Bertotti, A. novel approach for one-step fabrication of platinum-nanoporous gold film via oxygen bubble template with enhanced electrochemical activity, Electrochem. Commun. 100 (2019) 96–99.
[29] B.J. Plowman, L.A. Jones, S.K. Bhargava, Building with bubbles: the formation of high surface area honeycomb-like films via hydrogen bubble templated electrodeposition, Chem. Commun. 51 (2015) 4331–4346.
[30] T.A. Rebbecchi Junior, Y. Chen, Template-based fabrication of nanoporous metals, J. Mater. Res. 33 (2018) 2–15.
[31] A.A. Cardenas-Riojas, S.L. Calderon-Zavaleta, U. Quiroz-Aguinaga, E.O. López, M. Ponce-Vargas, A.M. Baena-Moncada, Evaluation of an electrochemical sensor based on gold nanoparticles supported on carbon nanofibers for detection of tartrazine dye, J. Solid State Electrochem. 27 (2023) 1969–1982.
[32] C.J. Weber, N.E. Strom, O. Simoska, Electrochemical deposition of gold nanoparticles on carbon ultramicroelectrode arrays, Nanoscale 16 (2024) 16204–16217.
[33] J. Ding, H. Zhang, F. Jia, et al., Assembly of carbon nanotubes on a nanoporous gold electrode for acetylcholinesterase biosensor design, Sens. Actuators B Chem. 199 (2014) 284–290.
[34] M. Regiart, A.M. Gimenez, R.F. Marques, et al., Microfluidic device based on electrodeposited nanoporous gold/carbon nanotubes for plasmodium vivax detection, Sens. Actuators B Chem. 340 (2021) 129961.
[35] S. Zhao, L. Wang, T. Wang, et al., A high-performance hydrazine electrochemical sensor based on gold nanoparticles/single-walled carbon nanohorns composite film, Appl. Surf. Sci. 369 (2016) 36–42.
[36] S.M. Khoshfetrata, M.A. Mehrgardi, Dual amplification of single nucleotide polymorphism detection using graphene oxide and nanoporous gold electrode platform, Analyst 139 (2014) 5192–5199.
[37] C. Tan, X. Huang, H. Zhang, Synthesis and applications of graphene-based noble metal nanostructures, Materials 16 (2013) 29–36.
[38] A.D. Silva, W.J. Paschoalino, J.P.V. Damasceno, L.T. Kubota, Structure, properties, and electrochemical sensing applications of graphene-based materials, ChemElectroChem 7 (2020) 4508–4525.
[39] S. Kumaran, P.R. Buvaneswari, K.V.M. Shree, V. Rajmohan, Fabrication of rGO-modified ternary metal chalcogenide hybrid nanocomposite(rGO/Cu2MnSnS4) for high-performance supercapacitors, Diamonds Relat. Mater. 148 (2024) 11384.
[40] M.N.L. de Camargo, M. Santhiago, C.M. Maroneze, et al., Tuning the electrochemical reduction of graphene oxide: structural correlations towards the electrooxidation of nicotinamide adenine dinucleotide hydride, Electrochim. Acta 197 (2016) 194–199.
[41] X. Niu, W. Pei, J. Ma, Medium entropy FeCoNi nanoalloy supported on reduced graphene oxide for efficient electrochemical detection roxarsone in food samples, Food Chem. 455 (2024) 139918.
[42] M. Regiart, A. Kumar, J.M. Gonçalves, et al., An electrochemically synthesized nanoporous copper microsensor for highly sensitive and selective determination of glyphosate, ChemElectroChem 7 (2020) 1558–1566.
[43] J. Wu, M. Lin, X. Cong, et al., Raman spectroscopy of graphene-based materials and its applications in related devices, Chem. Soc. Rev. 47 (2018) 1822–1873.
[44] L. Killedar, D. Ilager, et al., Fast and facile electrochemical detection and determination of fungicide carbendazim at titanium dioxide designed carbon-based sensor, Mater. Chem. Phys. 285 (2022) 126131.
[45] X. Chen, W. Li, C. Lu, et al., Highly sensitive electrochemical detection of carbendazim residues in water by synergistic enhancement of nitrogen-doped carbon nanohorns and polyethyleneimine modified carbon nanotubes, Sci. Total Environ. 851 (Part 2) (2022) 158324.
[46] X. Gao, Y. Gao, C. Bian, et al., Electroactive nanoporous gold driven electrochemical sensor for the simultaneous detection of carbendazim and methyl parathion, Electrochim. Acta 310 (2019) 78–85.
[47] Y. Yang, H. Tan, Y. Wang, et al., A novel electrochemical sensor for sensitive detection of carbendazim based on zeolitic-imidazolate-framework-67/carbon nanohorns nanocomposite, Mater. Res. Bull. 179 (2024) 112975.
[48] D.J. Hamilton, Á. Ambrus, R.M. Dieterle, A.S. Felsot, et al., Regulatory limits for pesticide residues in water (IUPAC Technical Report), Pure Appl. Chem 75 (2003) 1123–1155.
[49] M. Brycht, O. Vajdle, K. Sipa, et al., β-cyclodextrin and multiwalled carbon nanotubes modified boron-doped diamond electrode for voltammetric assay of carbendazim and its corrosion inhibition behavior on stainless steel, Ionics 24 (2018) 923–934.
[50] L. Wang, M. Li, B. Li, et al., Electrochemical sensor based on laser-induced graphene for carbendazim detection in water, Foods 12 (12) (2023) 2277.
[51] T. Lima, H.T.D. Silva, G. Labuto, F.R. Simões, L. Codognoto, An experimental design for simultaneous determination of carbendazim and Fenamiphos by electrochemical method, Electroanalysis 28 (2016) 817–822.
[52] R. Liu, B. Li, F. Li, et al., A novel electrochemical sensor based on β-cyclodextrin functionalized carbon nanosheets@carbon nanotubes for sensitive detection of bactericide carbendazim in apple juice, Food Chem. 384 (2022) 132573.
[53] M.A.P. Papi, M.F. Bergamini, L.H. Marcolino Junior, Electrochemical determination of carbendazim in juice samples using carbon composite electrode modified with ion-exchange resin, Electroanalysis 36 (2024) e202300205.
[54] Y. Tang, X. Zhan, J. Zheng, et al., Facile colorimetric smartphone-based biosensor for rapid detection of organophosphorus pesticides residues in environment using the aptamer-enhanced oxidase activity of octahedral Ag2O particles, Anal. Chim. Acta 1264 (2023) 341325.